

Quantum fluctuations and the exchange bias field

G. J. Mata and E. Pestana

Departamento de Física, Universidad Simón Bolívar, Apartado 89000, Caracas 1080A, Venezuela

Miguel Kiwi

Facultad de Física, Pontificia Universidad Católica de Chile, Casilla 306, Santiago, Chile

Hugues Dreyse

IPCMS - GEMME, 23, rue du Loess BP43, 67034 Strasbourg, Cedex 2, France

(Received 10 May 2006; published 6 October 2006)

Ground-state fluctuations reduce the zero-temperature magnetic moments of the spins in a quantum antiferromagnet. In the neighborhood of surfaces, interfaces, and other defects which break translational symmetry, these fluctuations are not uniform. Because of this, the magnetic moments of up and down spins do not exactly compensate each other—as they do in a bulk antiferromagnet. At a surface or interface this leads to a small magnetic dipole density. The corresponding dipole field can account for the magnitude of observed exchange anisotropies. At finite temperatures localized surface (interface) excitations are populated and change the dipole density, making the exchange field temperature dependent. In a pure antiferromagnet fluctuations may induce a net surface magnetization. This should be observable in clean surfaces, by means of surface-sensitive magnetic probes such as the magneto-optic Kerr effect.

DOI: [10.1103/PhysRevB.74.144407](https://doi.org/10.1103/PhysRevB.74.144407)

PACS number(s): 75.10.Jm, 75.45.+j, 75.60.-d, 75.70.-i

I. INTRODUCTION

Exchange anisotropy arises when two differently ordered magnetic materials, one ferro- and the other antiferromagnetic, being in contact, are cooled through their ordering temperatures in an external magnetic field. It has been observed, for example, in clusters or small particles, ferromagnetic (FM) films deposited on single-crystal or polycrystalline antiferromagnetic (AFM) substrates, FM or AF thin-film bilayers, and spin glasses. In these systems the center of the hysteresis loop is shifted by an amount called the exchange bias field. With the convention that the positive field direction is that of the cooling field, this exchange bias is, in most cases, negative.

Although exchange anisotropy has attracted the attention of physicists and materials scientists for almost half a century¹⁻⁴ and has resulted in extensive technological applications in the storage and sensor industries,⁵ a full understanding of its physical origin has not been achieved.

From the experimental results it is now certain that the effect is due to a fixed spin arrangement on the AFM side of the interface.⁶⁻⁸ However, the nature of this arrangement and the microscopic mechanism leading to the exchange bias field are still open questions. Most of the theoretical work has made use of the classical Heisenberg model in various forms,⁴ an exception being the contribution of Suhl and Schuller,⁹ who have interpreted the exchange field as a self-energy shift due to the emission and reabsorption of AFM spin waves. Recently, a theory based on the Dzyaloshinsky-Moriya interaction has been developed by Ijiri *et al.*¹⁰

In this paper we put forward the idea that quantum fluctuations lead to a two-dimensional dipole moment density in the AF. This, in turn, generates a dipolar field which can account for exchange bias anisotropy, and we argue here that exchange bias thus results from quantum fluctuations. Let us address this claim for the case of a two-sublattice antiferro-

magnet, for which the relevant order parameter is the staggered magnetization $\langle \hat{\mathbf{M}}_{AF} \rangle = g\mu_B \langle \sum_\alpha \hat{\mathbf{S}}_\alpha - \sum_\beta \hat{\mathbf{S}}_\beta \rangle$, where $\hat{\mathbf{S}}_\alpha$ and $\hat{\mathbf{S}}_\beta$ denote the spin operators at the spin-up and spin-down sublattices. If we assume a Heisenberg Hamiltonian $\mathcal{H} = \sum_{ij} J_{ij} \hat{\mathbf{S}}_i \cdot \hat{\mathbf{S}}_j$, we can see that $[\hat{\mathbf{M}}_{AF}, \mathcal{H}] \neq 0$, in other words, that $\hat{\mathbf{M}}_{AF}$ is not constant in time. Therefore its time-averaged value must be smaller than its maximum value, even at $T = 0$. [If N is the number of spins and $\sqrt{S(S+1)}$ is the spin magnitude, this maximum value is NS .] In a translationally invariant system the reduction of the magnetization is equally shared by all spins. Moreover, since the spin-up and spin-down sublattices are equivalent then $\langle \sum_\alpha \hat{\mathbf{S}}_\alpha \rangle = -\langle \sum_\beta \hat{\mathbf{S}}_\beta \rangle$, that is, the system magnetic moment is zero. But when translational symmetry is broken by surfaces, interfaces, or other defects, a net magnetic moment can appear because the decrease of spin-up averages need not equal the corresponding spin-down reduction.¹¹⁻¹⁴

In this paper we show how in an ideal FM-AFM interface such a net magnetic moment appears. The resultant magnetization is confined to the interface itself and may be regarded, in the continuum limit, as a two-dimensional dipole density. This dipole sheet produces a magnetic field which interacts with the moments in the FM and contributes an additional term to the magnetic energy. This additional energy term can explain exchange bias.

Our numerical results indicate that the magnitude of this magnetic moment is only a few percent of that of a single AFM spin, which leads to a magnetic anisotropy consistent with the experimental results.

II. IDEAL FERROMAGNETIC-ANTIFERROMAGNETIC INTERFACE

We now describe our model system, in which atomic spins of magnitude $\sqrt{S(S+1)}$ are located at the sites of a bcc

lattice. Our system is divided in two halves by a (001) interface. On one side of the interface, nearest-neighbor spins are coupled ferromagnetically by the exchange integral $-J_F$. On the other, nearest-neighbor spins are coupled antiferromagnetically by the exchange integral J_A . Across the interface, spins are coupled by the exchange integral $-J_0$.

We decompose the bcc lattice into planes parallel to the interface. In the AFM side, each of these planes is FM ordered and its spin direction alternates from one plane to the next; we group these planes into pairs and label each *pair* with the index $l \geq 0$, in such a way that $l=0$ labels the pair of planes closest to the interface; for each pair we label the corresponding planes with the subscript α for spins up, and the label β for spins down. In the FM side each index ($l < 0$) denotes a single, spin-up, layer. This choice of notation reflects the fact that in the AFM the unit cell is doubled. The Hamiltonian can be written as

$$\mathcal{H} = \sum_{l=0}^{+\infty} \sum_{\mathbf{R}, \delta} [J_{l,l} \mathbf{S}_\alpha(l, \mathbf{R}) \cdot \mathbf{S}_\beta(l, \mathbf{R} + \delta) + J_{l,l+1} \mathbf{S}_\beta(l, \mathbf{R} + \delta) \cdot \mathbf{S}_\alpha(l+1, \mathbf{R})] + \sum_{l=-\infty}^{-1} \sum_{\mathbf{R}, \delta} J_{l,l+1} \mathbf{S}_\alpha(l, \mathbf{R} + \delta) \cdot \mathbf{S}_\alpha(l+1, \mathbf{R}), \quad (1)$$

where $\mathbf{R} = a(n_1 \hat{\mathbf{x}} + n_2 \hat{\mathbf{y}})$ specifies a two-dimensional lattice point, a is the lattice constant, n_1 and n_2 are integers, $\delta = a(\pm \hat{\mathbf{x}} + \pm \hat{\mathbf{y}})$, and $\mathbf{S}_\alpha(l, \mathbf{R})$ [$\mathbf{S}_\beta(l, \mathbf{R})$] is a spin in the α (β) plane of the l th pair (and at site \mathbf{R} in that plane).

We use the Holstein-Primakoff transformation to rewrite the Hamiltonian in terms of boson operators a and b . Spin-wave interactions are neglected and therefore we discard quartic and higher-order terms. To take advantage of the in-plane translational symmetry we write boson operators as functions of the layer index l , and the two-dimensional wave vector \mathbf{k} . The Hamiltonian then decouples into a set of independent semi-infinite chains, each one corresponding to a wave vector \mathbf{k} . These chains are conveniently analyzed using Green functions, which we define as

$$G_{ll'}^{aa} = -\frac{i}{\hbar} \int_{-\infty}^{\infty} dt e^{i\omega t} \theta(t) \langle [a(l, \mathbf{k}, t), a^\dagger(l', \mathbf{k}, 0)] \rangle, \quad (2)$$

where $\langle A \rangle$ denotes the thermal average of A and the operators are in the Heisenberg picture. The functions $G_{ll'}^{bb}$, $G_{ll'}^{ab}$, and

$G_{ll'}^{ba}$ are defined in the same fashion. We use the transfer-matrix method^{20,21} to calculate these G 's. When the interface coupling is FM we find the following expressions for the diagonal elements of the Green function:

$$G_{ll}^{aa}(z, \mathbf{k}) = G_{AF}(z, \mathbf{k}) [1 - T_{AF}^{2l}(z, \mathbf{k}) f_R(z, \mathbf{k})], \quad l \geq 0, \quad (3)$$

$$G_{ll}^{bb}(z, \mathbf{k}) = G_{AF}(z, \mathbf{k}) [1 - T_{AF}^{2l+1}(z, \mathbf{k}) f_R(-z, \mathbf{k})], \quad l \geq 0, \quad (4)$$

$$G_{ll}^{aa}(z, \mathbf{k}) = G_F(z, \mathbf{k}) [1 - T_F^{2(l+1)}(z, \mathbf{k}) f_L(z, \mathbf{k})], \quad l \leq -1. \quad (5)$$

In these equations $G_{AF}(z, \mathbf{k})$ is the diagonal ($l=l'$) element of the bulk Greens function for the AFM. $G_F(z, \mathbf{k})$ is the diagonal element of the bulk Greens function for the FM. From these diagonal elements and the transfer matrices $T_{AF}(z, \mathbf{k})$ and $T_F(z, \mathbf{k})$ one readily obtains the full bulk Green functions. Physically the transfer matrices describe plane-wave propagation in one-dimensional chains. Indeed, it is possible to define a one-dimensional wave vector k_z by the relation $T = \exp(ik_z)$. The interference effects at the right and left sides of the interface are contained in the functions $f_R(z, \mathbf{k})$ and $f_L(z, \mathbf{k})$. More explicitly,

$$G_{AF}(z, \mathbf{k}) = \frac{z + 2J_A}{Q_A(z, \mathbf{k})}, \quad (6)$$

$$Q_A(z, \mathbf{k}) = (z^2 - 4J_A^2)^{1/2} (z^2 - 4J_A^2 + 4J_A^2 |\gamma_{\mathbf{k}}|^2)^{1/2}, \quad (7)$$

$$T_{AF}(z, \mathbf{k}) = \frac{1}{2J_A^2 |\gamma_{\mathbf{k}}|^2} [4J_A^2 - z^2 - 2J_A^2 |\gamma_{\mathbf{k}}|^2 + Q_A(z, \mathbf{k})], \quad (8)$$

$$G_F(z, \mathbf{k}) = \frac{1}{Q_F(z, \mathbf{k})}, \quad (9)$$

$$Q_F(z, \mathbf{k}) = [(z - 2J_F - 2J_F |\gamma_{\mathbf{k}}|)(z - 2J_F + 2J_F |\gamma_{\mathbf{k}}|)]^{1/2}, \quad (10)$$

$$T_F(z, \mathbf{k}) = \frac{1}{2J_F |\gamma_{\mathbf{k}}|^2} [2J_F - z + Q_F(z, \mathbf{k})], \quad (11)$$

$$f_R(z, \mathbf{k}) = \frac{(z - 2J_0 + Q_F)[(z + 2J_A)(z - 2J_0) - Q_A] - 4J_0^2 |\gamma_{\mathbf{k}}|^2 (z + 2J_A)}{(z - 2J_0 + Q_F)[(z + 2J_A)(z - 2J_0) + Q_A] - 4J_0^2 |\gamma_{\mathbf{k}}|^2 (z + 2J_A)}, \quad (12)$$

and

$$f_L(z, \mathbf{k}) = \frac{(z - 2J_0 - Q_F)[(z + 2J_A)(z - 2J_0) + Q_A] - 4J_0^2 |\gamma_{\mathbf{k}}|^2 (z + 2J_A)}{(z - 2J_0 + Q_F)[(z + 2J_A)(z - 2J_0) + Q_A] - 4J_0^2 |\gamma_{\mathbf{k}}|^2 (z + 2J_A)}. \quad (13)$$

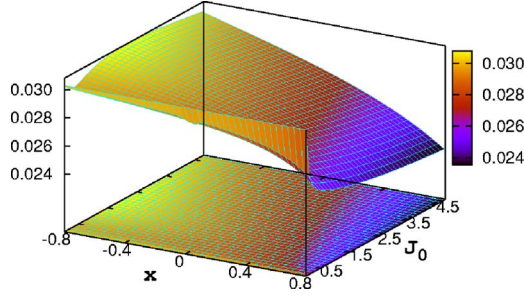


FIG. 1. (Color online) Net magnetization in the antiferromagnetic side of the interface as a function of $x=(J_F-J_A)/(J_F+J_A)$ and $J_0/(J_F+J_A)$. We choose units in which $J_F+J_A=1$. The coupling across the interface is ferromagnetic.

When the interface coupling is AFM we obtain very similar expressions, the only difference being that the exponents of T_{AF} in Eq. (8) and T_F in Eq. (11) are shifted by -1 and $+2$, respectively.

The average spin on plane l is given by

$$\langle S_{l,a}^z \rangle = S + \sum_{\mathbf{k}} \frac{1}{\pi} \text{Im} \int_{-\infty}^{\infty} d\omega \frac{G_{ll}^{aa}(\omega, \gamma_{\mathbf{k}})}{e^{\hbar\omega/k_B T} - 1}, \quad (14)$$

$$\langle S_{l,b}^z \rangle = -S - \sum_{\mathbf{k}} \frac{1}{\pi} \text{Im} \int_{-\infty}^{\infty} d\omega \frac{G_{ll}^{bb}(\omega, \gamma_{\mathbf{k}})}{e^{\hbar\omega/k_B T} - 1}. \quad (15)$$

The spectral distributions $\frac{1}{\pi} \text{Im}G$ in Eqs. (14) and (15) contain the contributions of interface and bulk excitations. The interface excitations are localized within a few layers of the interface. They appear for all values of the model parameters and dominate the spin reduction, and hence the net magnetization, at the interface. When $T=0$ the integrands in Eqs. (14) and (15) are zero for $\omega>0$. The negative ω -axis gives the effect of virtual spin waves on ground-state fluctuations.¹³ At finite temperatures real spin waves are excited which further change the net magnetization.

For our numerical calculations we choose units such that $J_F+J_A=1$. We use as our parameters J_0 and $x \equiv J_F-J_A$. In Fig. 1 we show the *net* magnetization in the AFM side of the interface, as a function of x and $J_0<0$. In Fig. 2 we show the corresponding results for $J_0>0$.

For this specific model we observe that the net magnetization per atom is of the order of a few percent. Is this a result that would be valid for other lattice structures and interfaces? Bulut *et al.*¹⁴ investigated the magnetization around a vacancy in a two-dimensional (2D) AFM. In this system all the spins in the n th neighboring shells point in the same direction. The average spins in the first and second shells give $\delta S \sim 0.03$, which is consistent with our results, but for a very different spin arrangement.

In addition, we notice that in these systems the correlation length, away from the critical points, is of the order of the interatomic distance. Therefore the results for the idealized interface studied here should hold for nonideal interfaces as well.

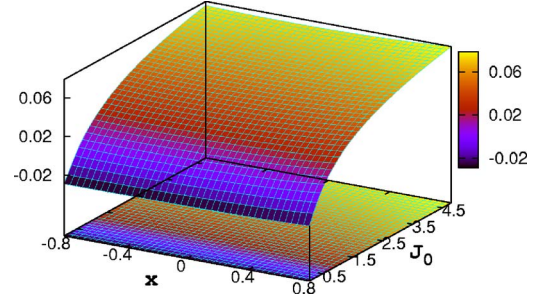


FIG. 2. (Color online) Net magnetization in the antiferromagnetic side of the interface as a function of $x=(J_F-J_A)/(J_F+J_A)$ and $J_0/(J_F+J_A)$. We choose units in which $J_F+J_A=1$. The coupling across the interface is antiferromagnetic.

Surface dipole density and exchange bias

The uncompensated antiferromagnetic spins give rise to a dipolar magnetic field \mathbf{B}_{AF} . This results in a Zeeman contribution to the energy density inside the FM, given by $-\mathbf{M}_F \cdot \mathbf{B}_{AF}$. \mathbf{M}_F is the FM magnetization field. This allows us to estimate the interface anisotropy energy per unit area, ΔE .^{2,3}

To this end we assume a circular AFM domain of radius R . On this domain there is a uniform dipole distribution $\sigma \sim 4g\mu_B\delta S/a^2$, due to the uncompensated fluctuations (here g is the gyromagnetic ratio, μ_B is the Bohr magneton, and a is the distance between neighboring spins). Adjacent to this domain there is a semi-infinite cylindrical ferromagnet, also of radius R . This FM is assumed to be in a single domain state, of magnetization M_F parallel to the interface and at angle ϕ with respect to the AFM positive axis. Integration of the Zeeman energy density over the cylinder yields

$$\Delta E = \alpha(M_F\mu_0g\mu_B\delta S/a^2)\cos\phi. \quad (16)$$

The constant α is the adimensional integral that results when distances are scaled by R and angles are scaled by 2π . Numerical computation yields $\alpha=0.47$.

With $\delta S \sim 10^{-2}$, $a \sim 0.1$ nm, and M_F equal to the saturation magnetization of Co, we find that $\Delta E \sim 0.08$ ergs/cm². In Table 2 of their review,³ Nogues and Schuller have compiled exchange anisotropy energies for oxide antiferromagnets used in exchange bias. For CoO, exchange anisotropy energies are typically in the range of $\sim 10^{-2}$ – $\sim 10^{-1}$ ergs/cm². This is consistent with our numerical estimate.

The free AFM surface is a special case, which corresponds to $J_0=0$, of the model investigated here. As can be seen in Figs. 1 and 2, this free surface also develops a net magnetization. Takano *et al.*¹⁵ have observed a thermoremanent magnetization at the free surface of CoO films that have been field cooled through the Néel temperature. They also studied bilayers of Ni₈₁Fe₁₉/CoO and found that the exchange bias field, after field cooling, has the same temperature dependence as the free film thermoremanent magnetization. This suggests that unidirectional anisotropy arises, as our model implies, due to the coupling between the FM and

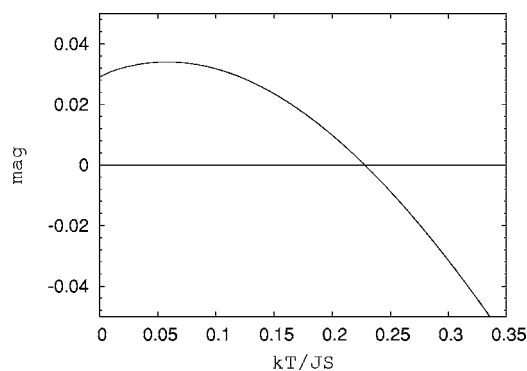


FIG. 3. Surface magnetization as a function of $k_B T / J_S$. To model the surface we take $J_0=0$.

the AFM *net* surface magnetization.

In nanoparticles, in which the surface to bulk ratio is significant, a surface magnetization can be observed. A net magnetization has indeed been reported in AFM ferritin¹⁶ and ferrihydrite¹⁷ nanoparticles.

To estimate the nanoparticle magnetization μ_p we use the formula

$$\mu_p = 6N_p^{2/3} g \mu_B \delta S, \quad (17)$$

where we have assumed that the nanoparticles are cubes containing N_p particles. We have also assumed that spin fluctuations are uniform on the nanoparticle surface. If we use the free surface value $\delta S=0.03$ and introduce the reported experimental values $N_p=4500$, for ferritin,¹⁶ and $N_p=2400$, for ferrihydrite,¹⁷ we find the estimates $\mu_p \sim 98\mu_B$, for ferritin, and $\mu_p \sim 65\mu_B$, for ferrihydrite. The experimental values are $345\mu_B$ and $250\mu_B$ for ferritin¹⁶ and ferrihydrite,¹⁷ respectively.

The temperature dependence of the exchange field can be explained as due to the thermal excitation of interface spin waves. In Fig. 3 we show the low-temperature variation of the net surface magnetization. For this particular geometry the surface magnetization reverses as the temperature increases. This changes the sign of the anisotropy energy and henceforth that of the exchange field. A sign reversal has been observed in field-cooled nanocrystalline bilayers of CoO and NiO/permalloy.¹⁸

The exchange bias field disappears at a temperature T_B , called the blocking temperature. For some systems T_B is considerably lower than the Néel temperature T_N . Since the energy bandwidth of interface spin waves is about half of that of bulk spin waves, they reach a considerable thermal population at a much lower temperature than bulk excitations. Thus we may conjecture that with rising temperature the surface disorders before the bulk. This would make the net surface magnetization, and therefore exchange bias, disappear below T_N . We must recall, however, that we have discarded quartic and higher-order terms. That is, we have used the noninteracting spin-wave approximation. This restricts the validity of our theory to temperatures low enough so that $|\delta S|/S \ll 1$ and precludes a quantitatively meaningful calculation of the blocking temperature.

Since the dipole interaction is long-ranged, the interface energy is sensitive to the configuration of the FM magnetization, \mathbf{M}_F . Here we have assumed that the FM is in a single-domain configuration, as is expected to be the case after cooling in a saturating field. If there were multiple domains in the FM, the unidirectional anisotropy would change. Gökemeijer *et al.*¹⁹ have shown that the state of the magnetization of the FM is, indeed, an essential parameter in establishing the exchange field; this, they also show, results in the exchange field being dependent on the accumulative memory of the thermal and applied field history of the sample.

III. SUMMARY AND CONCLUSION

In summary, we have put forward an alternative mechanism to generate exchange bias in a system where an antiferromagnet (AFM) is in contact with a metallic ferromagnet (FM). It differs from previously studied alternatives, since it is based on the fact that ground-state fluctuations reduce the zero-temperature magnetic moments of the spins in a quantum AFM, giving rise to an exchange field. In fact, in the vicinity of interfaces, and other defects which break translational symmetry, the above quantum fluctuations are not uniform. Because of this, the magnetic moments of up and down spins do not compensate exactly, as they do in a bulk AFM. Thus, close to a surface or interface, this leads to a small magnetic dipole density. At finite temperatures this exchange field becomes temperature dependent.

We have shown that this dipole field yields an interface energy which is in quantitative agreement with experimental results. In consequence, to further understand the exchange bias phenomenon, we suggest that studies of clean AFM surfaces by means of magnetization measurements, Brillouin light-scattering, and spin-polarized electron energy-loss spectroscopy could shed new light on the precise nature of the underlying mechanisms.

ACKNOWLEDGMENTS

M.K. was supported by the *Fondo Nacional de Investigaciones Científicas y Tecnológicas* (FONDECYT, Chile) under Grant No. 1030957. E.P. was partially supported by *Decanato de Investigaciones*, Universidad Simón Bolívar, Venezuela.

APPENDIX: CALCULATION OF ANISOTROPY ENERGY

Consider a very long cylindrical magnet of radius R . The bottom of this cylinder sits on the x - y plane. Its axis coincides with the positive z axis. It has a single FM domain with magnetization \mathbf{M} at angle φ from the x axis:

$$\mathbf{M} = M \hat{\mathbf{i}} \cos \varphi + M \hat{\mathbf{j}} \sin \varphi. \quad (A1)$$

On the bottom of the cylinder there is a two-dimensional layer with uniform dipole density:

$$\boldsymbol{\sigma} = -\sigma \hat{\mathbf{j}}. \quad (A2)$$

The position vector of a point at the dipole layer is expressed as

$$\mathbf{r}' = -\rho' \hat{\mathbf{i}} \sin \theta' + \rho' \hat{\mathbf{j}} \cos \theta'. \quad (\text{A3})$$

Likewise, the position vector of a point inside the cylinder is given by

$$\mathbf{r} = \boldsymbol{\rho} + z \hat{\mathbf{k}}, \quad (\text{A4})$$

where

$$\boldsymbol{\rho} = -\rho \hat{\mathbf{i}} \sin \theta + \rho \hat{\mathbf{j}} \cos \theta. \quad (\text{A5})$$

We define

$$\boldsymbol{\delta} = \mathbf{r} - \mathbf{r}'. \quad (\text{A6})$$

The contribution to the magnetic field at point \mathbf{r} due to a surface element at point \mathbf{r}' is

$$d\mathbf{B}_{fluct}(\mathbf{r}, \mathbf{r}') = -\frac{\mu_0}{4\pi} \sigma \rho' d\rho' d\theta' \frac{3\hat{\boldsymbol{\delta}}(\hat{\mathbf{j}} \cdot \hat{\boldsymbol{\delta}}) - \hat{\mathbf{j}}}{\delta^3}. \quad (\text{A7})$$

The corresponding contribution to the Zeeman energy per unit area is

$$dE_{fluct} = \frac{(\mathbf{M} d^3 r) \cdot d\mathbf{B}_{fluct}(\mathbf{r}, \mathbf{r}')}{\pi R^2}. \quad (\text{A8})$$

Upon integration over \mathbf{r} and \mathbf{r}' we find, after lengthy calculations, that the total energy per unit area is

$$E_{fluct} = \frac{\mu_0 \sigma M \cos \varphi}{8\pi^2 R^2} \int_0^R \rho' d\rho' \int_0^{2\pi} d\theta' \int_0^R \rho d\rho \int_0^{2\pi} d\theta \int_0^\infty dz \times \frac{1}{\delta^3} [\rho^2 + \rho'^2 - 2\rho\rho' \cos(\theta - \theta') - 2z^2]. \quad (\text{A9})$$

We now change the integration variables to $\varrho = \rho/R$, $\varrho' = \rho'/R$, $\vartheta = \theta/2\pi$, $\vartheta' = \theta'/2\pi$, $\zeta = z/R$. We also define $\eta = \delta/R$. The energy per unit area can be written as

$$E_{fluct} = \frac{\mu_0 \sigma M \cos \varphi}{2} I, \quad (\text{A10})$$

where

$$I = \int_0^1 \varrho' d\varrho' \int_0^1 d\vartheta' \int_0^1 \varrho d\varrho \int_0^1 d\vartheta \int_0^\infty d\zeta \frac{1}{\eta^3} \{ \varrho^2 + \varrho'^2 - 2\varrho\varrho' \cos[2\pi(\vartheta - \vartheta')] - 2\zeta^2 \}. \quad (\text{A11})$$

Numerical integration yields $I=0.98$.

-
- ¹W. H. Meiklejohn and C. P. Bean, Phys. Rev. **102**, 904 (1957).
²A. E. Berkowitz and K. Takano, J. Magn. Magn. Mater. **200**, 552 (1999).
³J. Nogués and I. K. Schuller, J. Magn. Magn. Mater. **192**, 203 (1999).
⁴M. Kiwi, J. Magn. Magn. Mater. **234**, 584 (2001).
⁵B. Dieny, V. S. Speriosu, S. S. P. Parkin, B. A. Gurney, D. R. Wilhoit, and D. Mauri, Phys. Rev. B **43**, R1297 (1991).
⁶H. Ohldag, T. J. Regan, J. Stohr, A. Scholl, F. Nolting, J. Luning, C. Stamm, S. Anders, and R. L. White, Phys. Rev. Lett. **87**, 247201 (2001).
⁷A. Hoffmann, J. W. Seo, M. R. Fitzsimmons, H. Siegwart, J. Fompeyrine, J.-P. Locquet, J. A. Dura, and C. F. Majkrzak, Phys. Rev. B **66**, 220406(R) (2002).
⁸H. Ohldag, A. Scholl, F. Nolting, E. Arenholz, S. Maat, A. T. Young, M. Carey, and J. Stohr, Phys. Rev. Lett. **91**, 017203 (2003).
⁹H. Suhl and I. K. Schuller, Phys. Rev. B **58**, 258 (1998).
¹⁰Y. Ijiri, J. Borchers, R. Erwin, T. Schulthess, and P. Van der Zaag (unpublished).
¹¹G. J. Mata and E. Pestana, in *New Trends in Magnetism, Magnetic Materials, and Their Applications*, edited by J. L. Morán López and J. M. Sanchez (Plenum, New York, 1994), pp. 201–209.
¹²G. J. Mata and E. Pestana, Phys. Rev. B **42**, 885 (1990).
¹³G. J. Mata and E. Pestana, Phys. Rev. B **31**, 7285 (1985).
¹⁴N. Bulut, D. Hone, D. J. Scalapino, and E. Y. Loh, Phys. Rev. Lett. **62**, 2192 (1989).
¹⁵K. Takano, R. H. Kodama, A. E. Berkowitz, W. Cao, and G. Thomas, Phys. Rev. Lett. **79**, 1130 (1997).
¹⁶Salah A. Makhlof, F. T. Parker, and A. E. Berkowitz, Phys. Rev. B **55**, R14717 (1997).
¹⁷M. S. Seehra, V. S. Babu, A. Manivannan, and J. W. Lynn, Phys. Rev. B **61**, 3513 (2000).
¹⁸C. Prados, E. Pina, A. Hernando, and A. Montone, J. Phys.: Condens. Matter **14**, 10063 (2002).
¹⁹N. J. Gökemeijer, J. W. Cai, and C. L. Chien, Phys. Rev. B **60**, 3033 (1999).
²⁰F. Yndurain, J. D. Joannopoulos, M. L. Cohen, and L. M. Falicov, Solid State Commun. **15**, 617 (1974).
²¹L. M. Falicov and F. Yndurain, J. Phys. C **8**, 147 (1975).